Progress In Electromagnetics Research Letters, Vol. 98, 95–103, 2021

A Low-F/D Wideband Transmitarray Antenna

Yan-Fang Liu[1], Lin Peng[1, *], Bo Wang[2], Wei-Sheng Yu[1], Tian-Cheng Zheng[1], and Xing Jiang[1]

Abstract—In this paper, a wide 3-dB gain bandwidth transmitarray (TA) antenna with low focal length to diameter ratio (F/D) is presented. The TA comprises four identical metasurface layers, and the metasurfaces are printed on thin dielectric substrates, which are separated by air gaps. The unit cells of the metasurfaces are constructed by etching slots on the metal layers, which include a serrated crevice and two disjunct slots. The F/D of the TA is designed as 0.48 to accommodate the applications required low profiles. A TA is constructed by arranging high transmission elements at the center and the other elements in the external of the aperture. A transmitarray antenna (TAA) operating at $9 \sim 13$ GHz is designed by applying a horn antenna to the TA, which achieves a measured 1-dB gain bandwidth of 10.5% (3-dB gain bandwidth of 23.3% and measured maximum gain of 22.48 dBi at 10.5 GHz) and a maximum measured aperture efficiency of 38.4%. Compared to the reported works, the proposed TA has outstanding F/D and wide 3-dB gain bandwidth.

1. INTRODUCTION

A transmitarray (TA), composed of many different elements arranged according to the specific phase compensation law, can be used to greatly improve the gain of the source antenna. Therefore, transmitarray antennas (TAAs) are very interesting in microwave and satellite communications, imaging, and radar systems [1–3]. Compared to convex lens, TAs have the advantages of planar and low-profile. However, it must be pointed out that the focal length to diameter ratios (F/D) of the TAs are usually large, which blemishes the advantage of low-profile. Therefore, low F/D TAs are very interesting for TAAs [4, 5].

For many TAAs, the distance between the source antenna and the TA is usually equivalent to the aperture of the TA, that is, $F/D \approx 1$ [6–8]. In [6], the TA is constructed by elements with different thicknesses, while its $F/D = 0.9$ ($D = 31$ cm). The TAA has a 1-dB gain bandwidth of 24.27% and maximum aperture efficiency of 62%. In [7], a quad-layer TA with double square loop elements is presented with $F/D = 0.95$ ($D = 32.19$ cm). The TAA achieves 1-dB gain bandwidth of 9.8% and maximum aperture efficiency of 50%. In [8], a TA with $F/D = 0.8$ ($D = 149.3$ mm) is designed using a four-layer double split ring slot structure. The measured 1-dB and 3-dB gain bandwidths are 7.4% and 17.7%, respectively, while its maximum aperture efficiency is 55%.

It is found from the above discussion that the TAA with large F/D has excellent aperture efficiency and bandwidth characteristics. However, for a low F/D TAA, it is difficult to obtain both the high aperture efficiency and wide bandwidth characteristics [9–11]. In [10], a TA with a low F/D of 0.3 is constructed by two-layer elements. The element is composed of a V-shaped pattern and metallic grating separated by a 0.127 mm Rogers 5880 substrate. The TAA achieves a 1-dB gain bandwidth of 4.3% and maximum aperture efficiency of 32%. In [11], a TA with fixed outer loop element is designed with

Received 12 May 2021, Accepted 10 June 2021, Scheduled 22 June 2021

* Corresponding author: Lin Peng (penglin528@hotmail.com).

[1] Guangxi Key Laboratory of Wireless Wideband Communication and Signal Processing, Guilin University of Electronic Technology, Guilin, Guangxi 541004, China. [2] Xi'an Electronic Engineering Research Institute, Xi'an, Shannxi 710100, China.

$F/D = 0.28$. The 1-dB gain bandwidth of the TAA is 6.3%, and the maximum aperture efficiency is 36.9%. It is found that the 1-dB gain bandwidths are narrow for the TAA with low F/D.

In this paper, a TA is designed by considering the F/D, bandwidth, and aperture efficiency. The TA has a low $F/D = 0.48$ ($F = 96$ mm). The proposed TAA achieves 1-dB gain bandwidth of 10.5% and 3-dB gain bandwidth of 23.3% with a maximum gain 22.48 dBi at 10.5 GHz. The maximum measured aperture efficiency is 38.4%.

2. TA AND UNIT CELL ELEMENT DESIGN

2.1. TA Design

As shown in Figure 1(a), a TA is expected to convert the spherical wave front of a source antenna to a plane wave, which means that the equiphase surface is a flat surface and perpendicular to the direction of propagation. Therefore, the TA should have the ability to compensate the phase of the arriving wave according to Equation (1) [12]

$$\phi_{ij}(x_i, y_j) = k_0\left(\sqrt{x_i^2 + y_j^2 + F^2} - F\right) \tag{1}$$

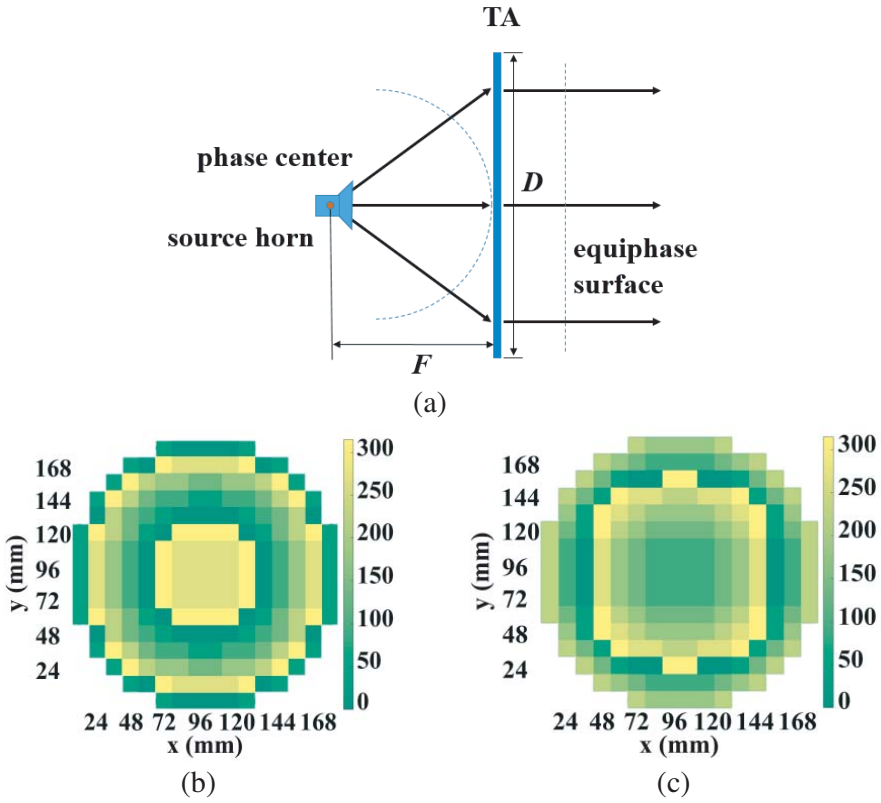

Figure 1. Phase requirements of the TA. (a) Schematic view of the TA. (b) Phase distribution calculated by Equation (1). (c) Phase distribution after modification.

In Equation (1), k_0 is the free space wave number at the center frequency; x_i and y_i are the position vector in Cartesian axes; and F is the assumed focal length.

It is found from Equation (1) that the compensated phases vary within the TA aperture, which require that the TA should be composed by elements with different phase responses. In our design, the compensation phase is quantized into 8 different values, i.e., the array contains 8 kinds of unit cell elements. The whole transmission array is discretized into 208 units. It is also found from Equation (1)

that a small F needs large phase compensating range for the aperture. In this research, the diameter of the aperture is set as 200 mm, and the F/D is set as 0.48. The phase distribution of the aperture is calculated by Equation (1) and presented in Figure 1(b). As a low F/D and wideband TAA is expected, the following factors that affect the broadband characteristics of TAA should be considered, such as magnitude loss effect, differential spatial phase effect, and phase error effect [7, 13, 14]. Therefore, the following strategy should be utilized to improve the performances. Firstly, as it is difficult to have all the 8 kinds of elements (with specific phase responses) to achieve high transmittances in a wide frequency band, and by also considering the fact that the elements at the center of the aperture receive more power from the source antenna, it is better to utilize elements with high transmission coefficient elements at the center. The elements in the center have 270° phase response from Equation (1); however, they have narrow high transmission bandwidth (from the simulated results in Figure 4). Therefore, in this design, the elements at the center are replaced by the elements with high transmission coefficient bandwidth, whose phase response is 90°. Then, the phase responses of the elements at the other positions should be changed in turn by the equation $\phi = \phi + 180°$. The phase distribution of the aperture in this design is shown in Figure 1(c). It is found that the compensating phases range from 0° to 315° in the TA aperture, which meet high requirement for the unit cell elements designing.

2.2. Unit Cell Design

From the above discussions, transmission coefficient and phase response of the unit cells of the TA will affect the bandwidth of the antenna, in which the elements should have transmission coefficient with high magnitude and specific phase responses. In other words, the characteristics of the elements are a critical factor for the performances of the TA. Resonant structures have prominent effects on the phase responses [15–18], which could be used in element designing. In the design of the unit cell, the dielectric substrate with $\varepsilon_r = 2.2$ is used. However, a very thin layer of substrate is used in order to minimize the dielectric loss. Multi-layer structure can be used to enhance the bandwidth of a TA antenna. In [13], a three-layer structure is used to improve the bandwidth characteristics. In [7, 8, 14], the proposed structures have 4 layers. In some of these researches, different structures or dimensions are utilized for different layers, which could increase the design complexity. In this research, a 4-same-layer structure is used to increase the bandwidth of the TA antenna. Each layer of the unit cell element is composed of a thin dielectric substrate of 0.254 mm and a metal layer. The elements are constructed by etching slots on the metal layers, which include a serrated crevice and two disjunct slots. As shown in Figure 2, the unit cell periodicity is $T = 12\,\text{mm} = 0.44\lambda$ ($f = 11\,\text{GHz}$). The spacing between the layers is $d = 6.535\,\text{mm} = 0.24\lambda$.

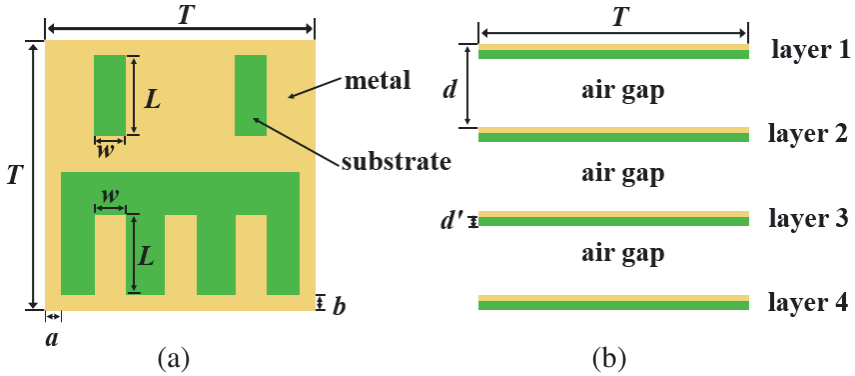

Figure 2. Geometry of the unit cell element. (a) Top view. (b) Side view.

As low F/D is desired, TA elements with large phase adjustable ability are required. Ulteriorly, the electric field should be concentrated on certain part of the element to endue a large phase adjustable ability. Therefore, the electric fields of 11 GHz are investigated as shown in Figure 3. It is found from the figure that there are strong field distributions in the serrated crevices, which indicates that

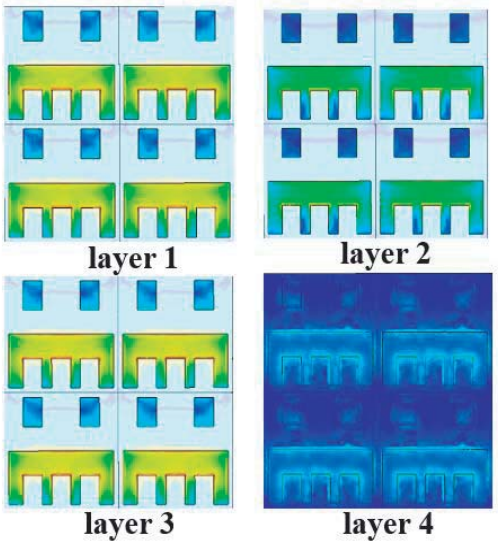

Figure 3. E-field of each layers of the element.

the serrated crevices have a great influence on the performance and large phase adjustable ability. Therefore, different transmission phase elements can be obtained by changing the parameters (L, a, b) of the serrated crevices.

In this design, eight units with different combinations of the parameters (L, a, b) of the serrated crevices were optimized as shown in Table 1. The results of the units are plotted in Figure 4(a) shows the phase response of the units, and Figure 4(b) demonstrates the phase differences (to the unit 3). It is found that, with different combinations of the parameters (L, a, b) of the serrated crevices, 315° transmission phase shift (9 GHz $\sim$ 13 GHz) is achieved. For most unit cells, the transmission phase changing is approximately linear with frequency, which is important for broadband performance of the antenna. However, as exhibited in Figure 4(c), the transmission coefficients of some of the elements are low at the low and high frequencies, which make poor gain performance at these frequencies. Fortunately, there are also some elements obtaining approximate 1 transmission coefficients at the whole frequency range. To abate the negative effects of the narrow transmission coefficient band elements, they are arranged at the edges of the TA, while the good transmission coefficient elements are arranged at the center part of the TA.

Table 1. Parameters of the unit cells.

unit	a (mm)	b (mm)	w (mm)	L (mm)
unit1	0.1	0.5	2	2.8
unit2	0.5	0.5	2	3
unit3	0.1	0.5	2	1.8
unit4	0.1	0.5	2	1
unit5	0.5	0.5	2	1.8
unit6	0.5	0.5	2	1.2
unit7	0.1	0.5	2	3.4
unit8	0.1	0.5	2	3.2

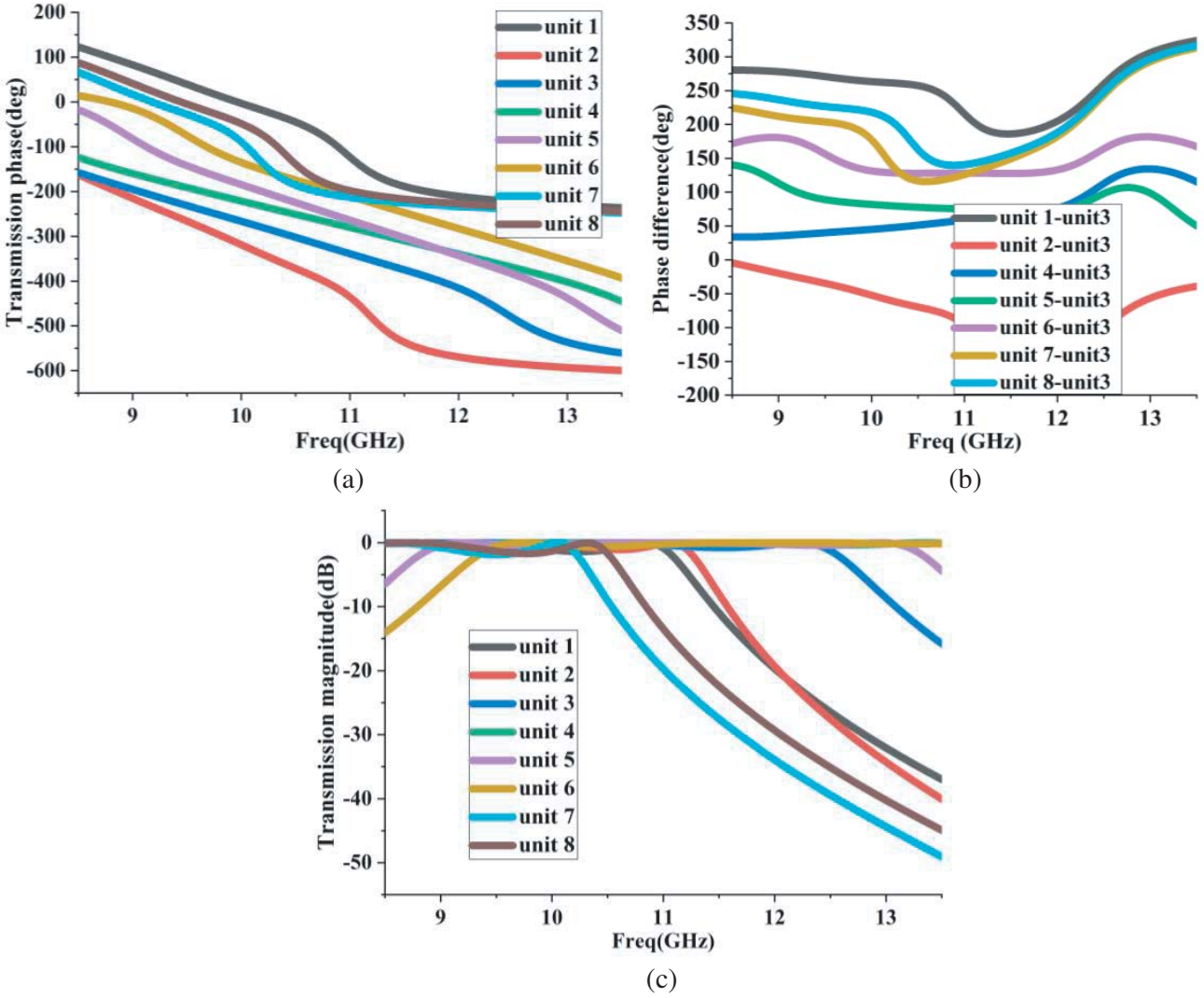

Figure 4. Transmission coefficient of different element at different frequency. (a) Phase. (b) Phase difference. (c) Magnitude.

3. PROTOTYPE FABRICATION AND MEASUREMENT

According to the above discussion, a prototype of the TA is fabricated with $F/D = 0.48$ ($F = 96\,\text{mm}$). The TA consists of 208 units in total. Four nylon columns and foam blocks are used to fix the four substrate layers. The feed source is a horn antenna, which has a simulation gain of 13.8 dBi at the center frequency of 11 GHz. The prototype antenna is simulated and measured as demonstrated in Figure 5.

The simulated and measured radiation patterns of the horn and the TAA in both E- and H-planes are demonstrated in Figures 6(a), (b), and (c) which exhibit the patterns of 9 GHz, 11 GHz, and 13 GHz, respectively. The cross polarization level is very low that the cross polarization level of E-planes is about -60 dB and H-planes about -20 dB. It is found from the figures that the simulated and measured radiation patterns are in good agreement with each other. Though there are some discrepancies between the simulated and measured radiation patterns, the beamwidths of the radiation patterns are successfully narrowed for all of the three frequencies as the TA is applied to the horn. As a result, significant gain performance enhancement can be expected. Compared to the horn, the TAA also has better side lobes.

The measured and simulated realized gain curves of the horn and TAA are plotted in Figure 7 for

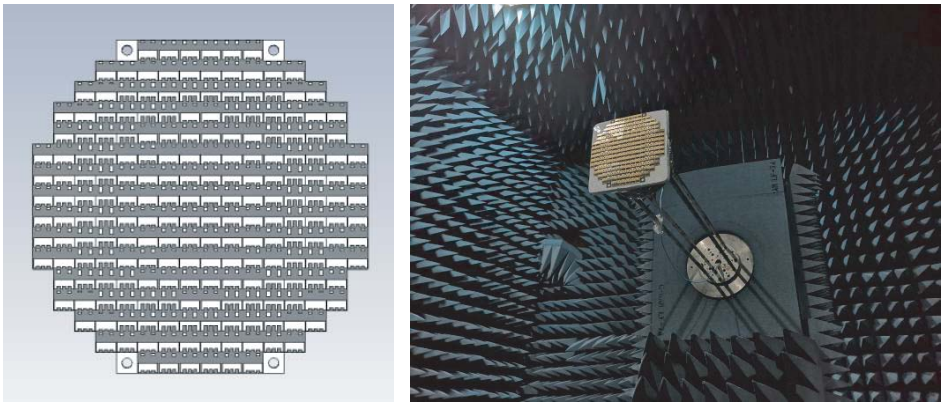

(a) (b)

Figure 5. The proposed TAA. (a) Simulated TA model. (b) Fabricated TAA and measurement.

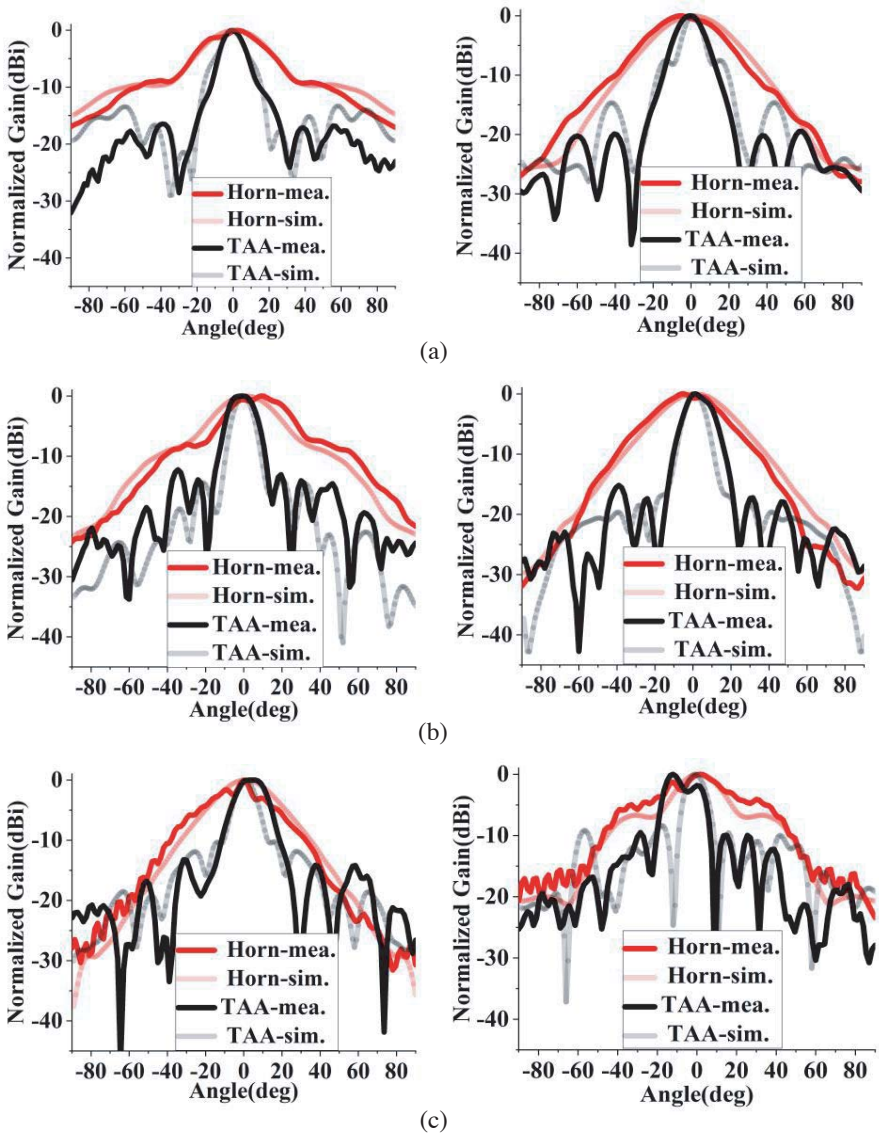

Figure 6. *E*-plane (left) and *H*-plane (right) patterns of the proposed TAA. (a) 9 GHz. (b) 11 GHz. (c) 13 GHz.

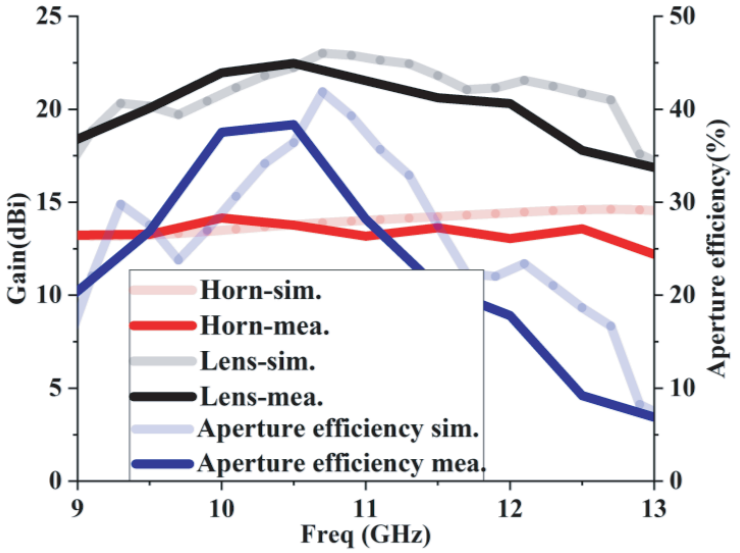

Figure 7. Measured and simulated realized gain and aperture efficiency of the proposed TAA.

comparison. It is found from the figure that the measured realized gains are enhanced by 4.2 dB to 8.7 dB in the 9–13 GHz band, while a peak gain of 22.48 dBi is obtained at 10.5 GHz. The simulation results show that the TAA achieves 1-dB gain bandwidth of 11% and 3-dB gain bandwidth of 32%. The measurement results show that the TAA achieves 1-dB gain bandwidth of 10.5% and 3-dB gain bandwidth of 23.3%, while a peak gain of 22.48 dBi is obtained at 10.5 GHz. The measured and simulated aperture efficiency curves of the TAA are also plotted in the figure. In the 9–13 GHz band, the maximum simulated and measured aperture efficiencies of the TAA are 42% and 38.4%, respectively.

The measured performances of the proposed TAA are compared to the reported TAA as exhibited in Table 2. Though References [7] and [8] have better maximum aperture efficiency than the proposed design, their F/D are larger. Moreover, the proposed TAA also has wider 1-dB and 3-dB gain bandwidths than [8]. For the TAAs of [13, 16, 17, 19], they have large F/D, smaller aperture efficiencies, and narrower 1-dB and 3-dB gain bandwidths. The TAAs in [11] also have small F/D (even smaller than the proposed design); however, their aperture efficiencies and 1-dB gain bandwidths are smaller than the proposed design.

Table 2. Comparison of the proposed TA with recent published designs.

Ref.	Freq. (GHz)	ε_{ap} (%)	1-dB gain BW	3-dB gain BW	F/D
[7]	13.5	50	9.8%	-	0.95
[8]	13.58	55	7.4%	17.7%	0.8
[11]	12	36.9	6.3%	-	0.3
[13]	11.3	30	9.0%	19.4%	0.8
[16]	11.3	16	4.2%	9.4%	0.8
[17]	10	36	4.0%	-	1
[19]	14.2	28.9	-	7.0%	1.5
This work	**11**	**38.4**	**10.5%**	**23.3%**	**0.48**

ε_{ap} (%) is aperture efficiency

4. CONCLUSION

In this paper, a TA with low $F/D = 0.48$ is proposed. The surfaces of the TA are identical, which could lower the design complexity. A wide phase coverage of 315° is obtained for the designed elements to compensate phase requirements of the TA aperture. Then, by arranging the elements with better performances in the center and the other elements in the external of the aperture, a TA is obtained. The TA is applied to a horn antenna, and the gain is enhanced by 4.2 dB to 8.7 dB in the 9–13 GHz, while the 1-dB and 3-dB gain bandwidths are 10.5% and 23.3%, respectively. The measured maximum aperture efficiency is 38.4%.

ACKNOWLEDGMENT

This work was supported in part by Innovation Project of Guangxi Graduate Education under Grant No. YCSW2020151, in part by GUET Excellent Graduate Thesis Program under Grant No. 18YJPYSS06, and in part by Key Laboratory of Cognitive Radio and Information Processing, Ministry of Education (Guilin University of Electronic Technology) under Grant No. CRKL190101.

REFERENCES

1. Federici, J. F., B. Schulkin, and F. Huang, "THz imaging and sensing for security," *Semicond. Sci. Technol.*, Vol. 20, No. 7, S266–S280, 2005.
2. Song, H. J. and T. Nagatsuma, "Present and future of terahertz communications," *IEEE Trans. Terahertz Sci. Technol.*, Vol. 1, No. 1, 256–263, Sep. 2011.
3. Yang, X., Y. Zhou, L. Xing, and Y. Zhao, "A wideband and low-profile transmitarray antenna using different types of unit-cells," *Microwave and Optical Technology Letters*, Vol. 61, No. 6, 1584–1589, 2019.
4. Menzel, W., D. Pilz, and M. Al-Tikriti, "Millimeter-wave folded reflector antennas with high gain, low loss, and low profile," *IEEE Antennas Propag. Mag.*, Vol. 44, No. 3, 24–29, Jun. 2002.
5. Rahmati, B. and H. R. Hassani, "Low-profile slot transmitarray antenna," *IEEE Trans. Antennas Propag.*, Vol. 63, No. 1, 174–181, Jan. 2015.
6. Ramazannia Tuloti, S. H., P. Rezaei, and F. Tavakkol Hamedani, "High-efficient wideband transmitarray antenna," *IEEE Antennas Wireless Propag. Lett.*, Vol. 17, No. 5, 817–820, May 2018.
7. Abdelrahman, A. H., P. Nayeri, A. Z. Elsherbeni, and F. Yang, "Bandwidth improvement methods of transmitarray antennas," *IEEE Trans. Antennas Propag.*, Vol. 63, No. 7, 2946–2954, Jul. 2015.
8. Liu, G., H. Wang, J. Jiang, F. Xue, and M. Yi, "A high-efficiency transmitarray antenna using double split ring slot elements," *IEEE Antennas Wireless Propag. Lett.*, Vol. 14, 1415–1418, 2015.
9. Liu, S. L., X. Q. Lin, Z. Q. Yang, Y. J. Chen, and J. W. Yu, "W-band low-profile transmitarray antenna using different types of FSS units," *IEEE Trans. Antennas Propag.*, Vol. 66, No. 9, 4613–4619, Sept. 2018.
10. Yi, H., S. W. Qu, and C. H. Chan, "Low-cost two-layer terahertz transmitarray," *Electron. Lett.*, Vol. 53, No. 12, 789–791, Jun. 2017.
11. Wu, G., S. Qu, and S. Yang, "Low-profile transmitarray antenna with cassegrain reflectarray feed," *IEEE Trans. Antennas Propag.*, Vol. 67, No. 5, 3079–3088, May 2019.
12. Liu, X., L. Peng, Y. F. Liu, et al., "Ultra-broadband all dielectric transmitarray designing based on genetic algorithm optimization and 3D print technology," *IEEE Trans. Antennas Propag.*, Vol. 69, No. 4, 2003–2012, 2020.
13. Abdelrahman, A., H. A. Z. Elsherbeni, and F. Yang, "High gain and broad-band transmitarray antenna using triple-layer spiral dipole elements," *IEEE Antennas Wireless Propag. Lett.*, Vol. 13, 1288–1291, Jul. 2014.
14. Ryan, C. G. M., M. R. Chaharmir, J. Shaker, et al., "A wideband transmitarray using dual-resonant double square rings," *IEEE Trans. Antennas Propag.*, Vol. 58, No. 5, 1486–1493, May 2010.

15. Gao, S. S., S Sun, J. L. Li, and T. Yan, "Compact dual-mode dual-band bandpass filter with inside-outside-reversed dual-ring topology," *Electron. Lett.*, Vol. 53, No. 9, 624–626, Apr. 2017.
16. Abdelrahman, A. H., A. Z. Elsherbeni, and F. Yang, "Transmitarray antenna design using cross slot elements with no dielectric substrate," *IEEE Antennas Wireless Propag. Lett.*, Vol. 13, 177–180, 2014.
17. Tian, C., Y. Jiao, and G. Zhao, "Circularly polarized transmitarray antenna using low-profile dual-linearly polarized elements," *IEEE Antennas Wireless Propag. Lett.*, Vol. 16, 465–468, 2017.
18. Gao, S. S. and S. Sun, "Synthesis of wideband parallel-coupled line bandpass filters with non-equiripple responses," *IEEE Microw. Wireless Components Lett.*, Vol. 24, No. 9, 587–589, Sept. 2014.
19. Cai, Y., K. Li, S. Gao, et al., "Dual-band circularly polarized transmitarray with single linearly polarized feed," *IEEE Trans. Antennas Propag.*, Vol. 68, No. 6, 5015–5020, Jun. 2020.